

Water Cycle Algorithm (WCA): A New Technique to Harvest Maximum Power from PV

Original

Water Cycle Algorithm (WCA): A New Technique to Harvest Maximum Power from PV / Javed, M.Y., Hasan, A., Rizvi, S.T.H., Hafeez, A., Sarwar, S., Telmoudi, A.J.. - In: CYBERNETICS AND SYSTEMS. - ISSN 0196-9722. - ELETTRONICO. - (2022), pp. 80-102. [10.1080/01969722.2021.2008683]

Availability:

This version is available at: 11583/2948216 since: 2022-02-18T13:00:27Z

Publisher:

Taylor and Francis Ltd.

Published

DOI:10.1080/01969722.2021.2008683

Terms of use:

This article is made available under terms and conditions as specified in the corresponding bibliographic description in the repository

Publisher copyright

Taylor and Francis postprint/Author's Accepted Manuscript

This is an Accepted Manuscript of an article published by Taylor & Francis in CYBERNETICS AND SYSTEMS on 2022, available at <http://www.tandfonline.com/10.1080/01969722.2021.2008683>

(Article begins on next page)

Water Cycle Algorithm (WCA): A New Technique to Harvest Maximum Power from PV

Muhammad Yaqoob Javed, Ali Hasan, Syed Tahir Hussain Rizvi, Annas Hafeez, Sajid Sarwar, and Achraf Jabeur Telmoudi

QUERY SHEET

This page lists questions we have about your paper. The numbers displayed at left are hyperlinked to the location of the query in your paper.

The title and author names are listed on this sheet as they will be published, both on your paper and on the Table of Contents. Please review and ensure the information is correct and advise us if any changes need to be made. In addition, please review your paper as a whole for typographical and essential corrections.

Your PDF proof has been enabled so that you can comment on the proof directly using Adobe Acrobat. For further information on marking corrections using Acrobat, please visit <http://journalauthors.tandf.co.uk/production/acrobat.asp>; <https://authorservices.taylorandfrancis.com/how-to-correct-proofs-with-adobe/>

The CrossRef database (www.crossref.org/) has been used to validate the references.

AUTHOR QUERIES

- Q1** Please check if author names and affiliations have been typeset correctly and correct if inaccurate.
- Q2** Please provide location of the conference.
- Q3** Please provide the volume number and journal title.
- Q4** Please note that numbered references have been changed to name and year references as per journal style. Please check.



Water Cycle Algorithm (WCA): A New Technique to Harvest Maximum Power from PV

Q1 Muhammad Yaqoob Javed^a, Ali Hasan^a, Syed Tahir Hussain Rizvi^b,
Annas Hafeez^a, Sajid Sarwar^a, and Achraf Jabeur Telmoudi^c

^aDepartment of Electrical and Computer Engineering, COMSATS University Islamabad, Lahore Campus, Lahore, Pakistan; ^bDipartimento Di Elettronica E Telecomunicazioni, Politecnico di Torino, Torino, Italy; ^cLISIER Laboratory, The National Higher Engineering School of Tunis (ENSIT), University of Tunis, Tunis, Tunisia

ABSTRACT

Renewable energy or alternative energy is extracted through renewable resources. These are considered as an alternative from conventional fossil fuel-based sources because conventional energy sources are depleting rapidly and raised concerns over increasing environmental impacts. Among many renewable sources, solar energy has a substantial part to meet the increased energy demand with reduced environmental effects. Solar irradiance and temperature are key factors upon which photovoltaic (PV) power generation depends but its optimum operating point gets affected by variation in the above-mentioned environmental factors. Finding the optimum operating point is a challenge due to the nonlinear solar behavior and varying nature of environmental conditions. To overcome these challenges, maximum power point (MPP) searching algorithms are exploited to get optimum power from the PV energy system. Maximum power point tracking (MPPT) behavior is different for various weather conditions, for instance, partial shading (PS), and uniform irradiance (UI) conditions. Numerous MPPT methods came to be used to find the optimum power. This work deals with the development of a novel technique for MPP finding of a PV system on the basis of the Water Cycle Algorithm (WCA) under PS conditions. It turns out to be good in terms of exploration and exploitation. Thus, it has the capability to avoid getting stuck in local minima (LM) and to find the global maxima (GM). The performance of the CSA technique is examined on five different types of P-V patterns for UI and PS conditions through MATLAB simulation and experimental setup. The findings of WCA are equated with the previous well-known soft computing methods such as PSO, ACS, DFO, and conventional method P&O to evaluate performance. The outcomes reveal that the WCA algorithm overtakes P&O from the perspective of robustness, accuracy, efficiency, and stability, as well as PSO in respect of converging speed and efficiency.

KEYWORDS

MPPT; partial shading condition; Perturb and Observe (P&O); photovoltaic (PV); water cycle algorithm (WCA)

Introduction

Power generation from Solar is one of the most promising available renewable energy sources (RES). Which is clean, abundant, and inexhaustible of all RES to date. The sun radiates energy at the rate of 3.8×10^{20} MW and around 1.8×10^{11} MW is captured by the earth. Installed solar electricity capacity is approximately 227 GW by the end of 2015, equivalent to producing 1.9% of the electricity used globally (Renewables 2018).

Photovoltaic cells are used to convert solar energy using the principles of photovoltaic effect which is based on the interaction of light with photovoltaic materials, with absorbed photon energy greater or equal to the material's bandgap. PV energy systems have nonlinear behavior in nature and distinctive algorithm are needed to find maximum obtainable power through the PV arrays. The PV module's nonlinear features have a single MPP (Zhang et al. 2018). Solar irradiance and temperature are key factors upon which PV power generation depends. Multiple techniques have been developed to obtain optimum points and these techniques are known as MPP searching techniques. Solar irradiance is dependent on sunlight direction, shade produced by birds, clouds, buildings, and trees, etc. These partial shading conditions or fast-changing environments change MPP and thus highly affect the output power of the solar system (Aouchiche et al. 2018).

MPPT techniques may either be categorized as indirect and direct Methods. Direct approaches include procedures that measure PV current or voltage and also are independent of prior information on PV characteristics. So operating point of PV is independent of irradiance and temperature or degradation level (Karami, Moubayed, and Outbib 2017). The indirect methods are those methods that are based on parameters database including power and voltages curves of photovoltaic systems for various temperatures and irradiance, or the estimation of the MPP using mathematical functions derived through experimental data. Indirect methods use outside signals for estimation of the MPP and outside signals are typically given by measuring the short-circuit current (SCC), temperature, irradiance, and open-circuit voltage (OCV) from the PV array. MPP is derived from the monitored signal given by a set of parameters (Mohapatra et al. 2017).

MPPT methods may further be classified into classical or conventional and intelligent algorithms. Incremental Conductance (InC) and Perturb and Observe (P&O) are generally exploited conventional MPPT techniques. These techniques are fast, simple, and accurate under uniform shading conditions but their major disadvantage is that they failed to do so under PS conditions and get stuck into local maxima. Another disadvantage of this

87 technique is that they are not efficient because they keep oscillating around
88 MPP[4]. PV systems also employ offline techniques, for instance, fractional
89 open-circuit voltage (FOCV) and fractional short circuit current (FSCC),
90 which are low-cost and simple to deploy. The basic idea behind FOCV is
91 that MPP is mostly located among 0.70 to 0.82 of the OCV and for FSCC
92 this fraction is between 0.8 to 0.9 of the SCC (Karami, Moubayed, and
93 Outbib 2017). The key disadvantages of these methods are that it suffers a
94 periodic loss of power while measuring OCV or SCC and fail to perform
95 well under PS conditions. To enhance the above-mentioned procedures,
96 various adaptive and hybrid MPP searching approaches have been created.
97 Under uniform and quickly varying environmental conditions, these strat-
98 egies operate well, but not in PS scenarios. Furthermore, various hybrid
99 strategies were useful in locating the MPP. In order to increase PV energy
100 system performance, the hybrid mechanism combines traditional MPPT
101 methods with certain optimization approaches (Harrag and Messalti 2015).

102 Optimization and intelligent computational approaches based on
103 Artificial Intelligence (AI) are used to illustrate the shortcomings of trad-
104 itional MPPT approaches. These techniques include Artificial Neural
105 Networks (ANN) (Bouselham et al. 2017), Fuzzy Logic Controller (FLC)
106 (Yilmaz, Kircay, and Borekci 2018), and Evolutionary algorithms, for
107 instance, Particle Swarm Optimization technique (PSOT) (Babu, Rajasekar,
108 and Sangeetha 2015), Ant Colony Optimization method (ACOM) (Ram,
109 Babu, and Rajasekar 2017), and Genetic Algorithm (GA) (Daraban,
110 Petreus, and Morel 2013). They may be employed on their independently
111 or in combination with other traditional approaches. Such algorithms are
112 complex and slow but advancement in computers give good opportunities
113 to integrate these algorithms in real-time problems but they still have the
114 disadvantage of not implementing in the low-cost microcontroller. So far
115 no such method has been developed to address all these issues so we can-
116 not say about the best technique in MPPT.

117 The advantage of the MPPT based on PSO presented in (Ishaque et al.
118 2012) is to direct calculates the duty cycle and eliminate the necessity for
119 control loops PI. PSO method is built on an optimized search strategy that
120 removes the limitations of traditional approaches to locate global MPPT in
121 PS environments. But the method is complex and requires high processing
122 power to compute. For MPPT, a neural network-based InC technique is
123 developed (Punitha, Devaraj, and Sakthivel 2013). Artificial NN is trained
124 through a backpropagation method to estimate online reference voltage.
125 But required a long training time for deep networks, the complex architec-
126 ture required more processing power. P&O algorithm implanted in GA
127 and making a single algorithm result in reduced algorithm parameters and
128 required less iteration for MPPT (Daraban, Petreus, and Morel 2014).
129

130 This research work presents a new nature-inspired metaheuristic
131 algorithm used to find MPPT. Many studies have been conducted utilizing
132 WCA to solve various optimization challenges. WCA was exploited
133 by Navid Ghaffarzade in (Ghaffarzadeh 2015) to improve the variables of
134 power system stabilizers that are exploited to reduce the oscillations of
135 the power system. In (Haroon and Malik 2017), the authors applied
136 WCA to hydrothermal coordination problems to get their optimum
137 mutual operation.

138 The proposed solution is an indirect method of MPPT, a population-
139 based, nature-inspired metaheuristic optimization algorithm for resolving
140 different optimization issues. The WCA is a technique motivated by nature
141 and based on a hydrologic cycle that how water flows in streams and then
142 streams flows into rivers and then finally downhill location into a sea (opti-
143 mum point) (Eskandar et al. 2012). The best raindrop is picked through
144 the sea, followed by some other fine raindrops in the form of rivers, and
145 finally all rest as streams. The performance of an MPPT technique is based
146 on accuracy, convergence speed and steady-state error, complexity, number
147 of sensors used, and robustness and the proposed WCA technique can find
148 the optimum point while fulfilling the above-mentioned criteria
149 (Ghaffarzadeh 2015). The main advantages of the WCA are summarized
150 as follow:
151

- 152 • It needs less Number of Function Evaluations (NFEs = No. of
153 Iterations*Initial Population) to successfully track global MPP under
154 partial shading and dynamic environmental conditions.
- 155 • Once comes to steady-state it does not oscillate around the MPP so
156 power loss is prevented.
- 157 • It has a very low computational cost so, it could be executed in a low-
158 cost microcontroller.
- 159 • It needs relatively less time to track MPP than other intelligent techni-
160 ques i.e. its convergence speed is high.

161 **Partial Shading Problem**

162 PV arrays consist of series or parallel PV modules or a combination of
163 both. In the open atmosphere, some modules likely experience different
164 irradiance than other modules in the array, and this uneven irradiance on
165 different modules is referred to as Partial shading conditions (PSC). PS
166 happens because of the shade of the neighboring building, trees, or clouds.
167 Modules receiving high irradiance levels can be referred to as insolated
168 modules and modules receiving low irradiance levels can be referred to as
169 shaded modules. In series joined PV modules, shaded modules provide less
170
171
172

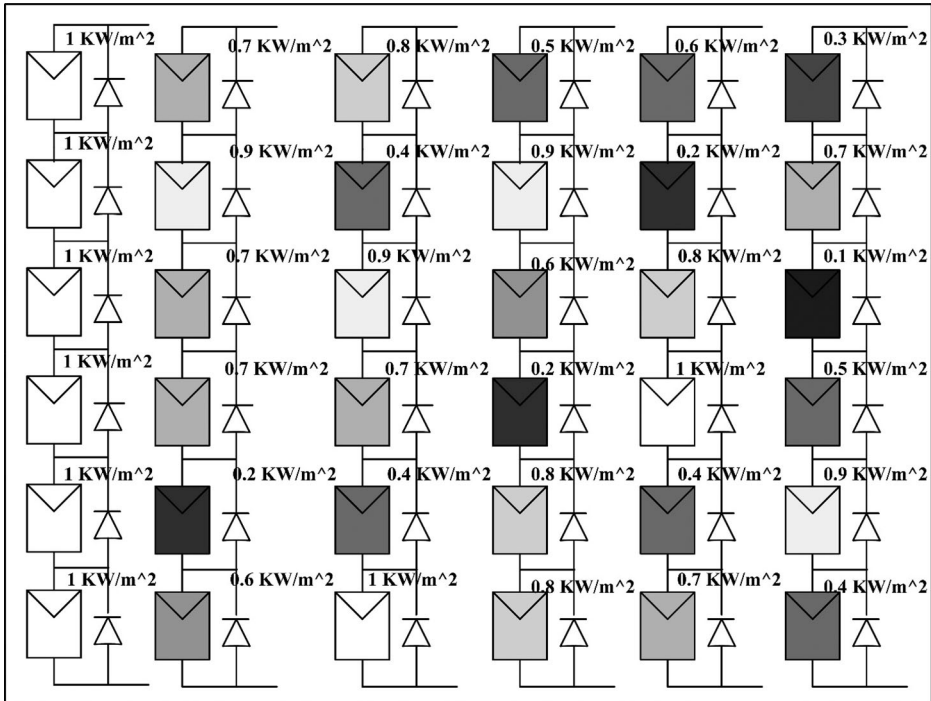
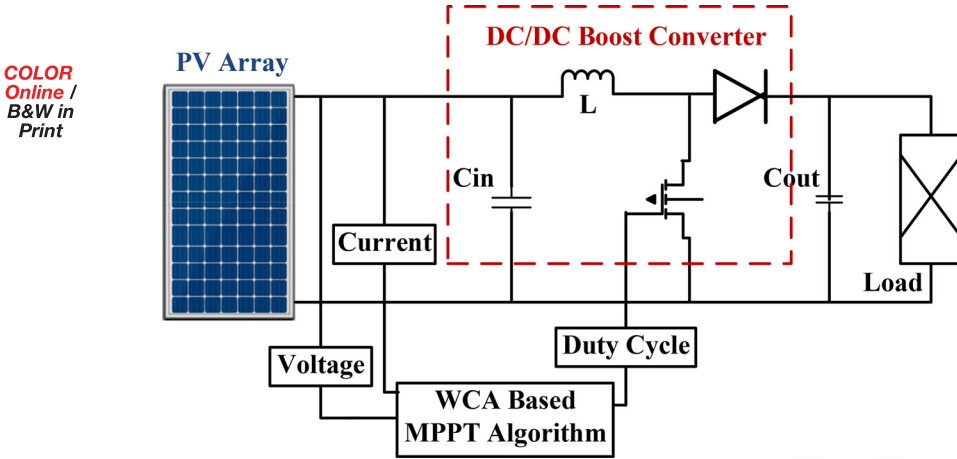


Figure 1. Series connected PV modules with by-pass diodes.

current than insolated modules. So the insolated modules drive the current in the array. A current larger than the PS module's current travels via the shaded module's shunt resistance, resulting in a negative voltage around the shaded modules and consume power rather than generate energy. This situation adversely affects the performance and efficiency of the PV system and damage PV models by creating hotspots and eventually damaging the modules because the shaded PV module behaves like a power sink and excess power dissipation in the module can irreparably damage the plastic cell encapsulation. To evade this situation, bypass diodes are linked in series with modules to provide an extra channel for current to flow, and thus improving the efficiency (Ghasemi, Foroushani, and Parniani 2016). Figure 1 shows five series-connected PV modules below UI and PS scenarios. Under UI all diodes operate in reverse biased so have no voltage drop but under different irradiance levels diode connected with shaded modules operates in forwarding bias causing the current to pass through the by-pass diode and thus experiencing a voltage drop.

In this study, a PV model has been developed and proposed WCA-based MPPT technique and one of the other well-known soft computing technique PSO was fed with identical models, and a comparative study was conducted for UI and various PS schemes. The results suggest that WCA outperforms than PSO algorithm for convergence speed.



229 **Figure 2.** PV Model.

230 **Modeling of PV System**

231 A complete PV model is shown in Figure 2. The load is being fed by a
232 boost converter and is being governed by a WCA-based MPP tracking con-
233 troller. Several models have been established to simulate the properties of
234 photovoltaic cells. A model of the single diode is employed for simulation.
235

236 **Single Diode Model PV Module**

237 A diode can be utilized to model the PV cell characteristics as demon-
238 strated in Figure 3. Ideally, a PV cell may be denoted by a diode and a
239 source of current. However, the practical model can also be realized by
240 incorporating two resistances R_S and R_{SH} into an ideal model, which
241 accounts for the leakage current inside the PV cell and on the borders.
242 Practically, the model is a fair tradeoff among simplicity and accuracy The
243 calculated equations of practical models are as given below:
244

$$245 I = I_{ph} - I_0 \exp \left(\left(\frac{q(V + IR_s)}{AKT} \right) - 1 \right) - \frac{V + IR_s}{R_{SH}} \quad (1)$$

$$246 I_{ph} = (I_{ph,n} + K_I \Delta T) \frac{G}{G_n} \quad (2)$$

$$247 I_0 = I_{0,n} \left(\frac{T_n}{T} \right)^3 \exp \left[\frac{qE_g}{ak} \left(\frac{1}{T_n} - \frac{1}{T} \right) \right] \quad (3)$$

250 where I_{ph} is light generated current, I_0 represents the saturation current of
251 the diode, q denotes the electronic charge and their value is taken
252 (1.6×10^{-19} C), K describes the Boltzmann constant, T illustrates the tem-
253 perature, and the ideality factor of a diode represents by A that usually has
254 a value between 1 and 1.5 [19]. $I_{ph,n}$ depicts the light- originated current at
255
256
257
258

COLOR
Online /
B&W in
Print

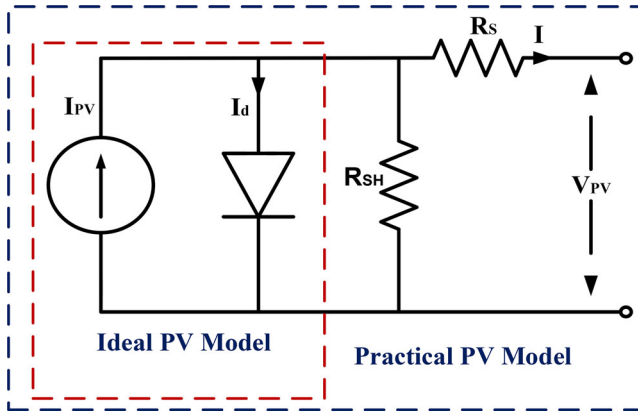


Figure 3. Diagram illustration of Single Diode PV model.

standard testing condition (STD) normally considered temperature at 25°C and G of 1000 W/m^2 , and $\Delta T = T - T_n$ (T_n and T presents the nominal and actual temperatures [in Kelvin], correspondingly). Where E_g reveals the semiconductor's bandgap energy.

Boost Converter

Boost converter's 'D' is the primary control method for regulating the voltage V_{pv} of the selected PV array. It is an important part of the PV system to work V_{pv} at GM. An input or primary side inductor (L_i), a switch (IGBT/MOSFET), a diode, and output or secondary side (C_o) capacitor are represented in Figure 4. The mathematical relation for duty cycle is given as:

$$\frac{V_{bt}}{V_{pv}} = \frac{I_{bt}}{I_{pv}} = \sqrt{\frac{R_o}{R_{in}}} = \frac{1}{1 - D} \quad (4)$$

Here, V_{bt} and I_{bt} represents the output voltage and current respectively of the power boost converter. I_{pv} and V_{pv} denotes the current and voltage of the PV module correspondingly.

Water Cycle Algorithm (WCA)

Basic Concept: For tackling optimization issues, a population-based optimization method is used. The WCA is a technique motivated by nature and based on a hydrologic cycle that how water flows in streams and then streams flows into rivers and then finally downhill location into a sea (optimum point). To understand it further, consider how water evaporates into the atmosphere and condenses into a colder environment, and then comes back to earth in rainfall. This water together with snowmelt starts its

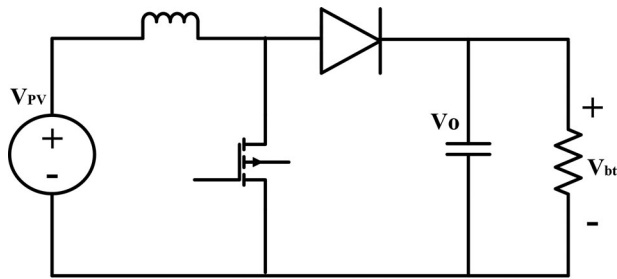


Figure 4. Basic Boost converter diagram.

journey up into the mountains through small streams which make up rivers and then finally end up into the sea. The best raindrop is designated by means of sea, while some further superb drops of rain are recognized by way of rivers. and all others are chosen as streams. Water Cycle Algorithm can find the maxima or minima of a function with good speed and accuracy (Sadollah et al. 2015).

Figures 5 and 6 show a real-world example of the Hydrological process and schematic view of the process respectively.

WCA for MPPT

MPP tracking using WCA is started by generating randomly generating voltage sample using the below equation:

$$V^i = LB + rand \times (UB - LB) \quad i = 1, 2, \dots, N_{pop} \quad (5)$$

$$V^i = \begin{bmatrix} V^1 \\ V^2 \\ \vdots \\ V^{N_{pop}} \end{bmatrix} \quad (6)$$

Then calculate the power against each voltage point.

$$P^i = \begin{bmatrix} P^1 \\ P^2 \\ \vdots \\ P^{N_{pop}} \end{bmatrix} \quad (7)$$

The initial population of the voltage points is then referred to as streams, river, and sea which are current position, local and global best voltage points based on the power at corresponding voltage points measured from PV array. A specific number of current-voltage points are directly compared with local and global best points based on the following equation:

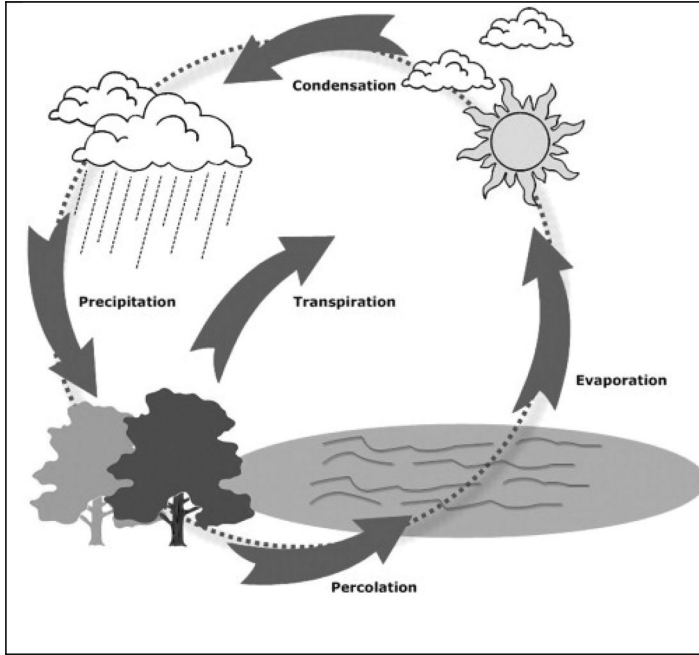


Figure 5. Hydrological Cycle.

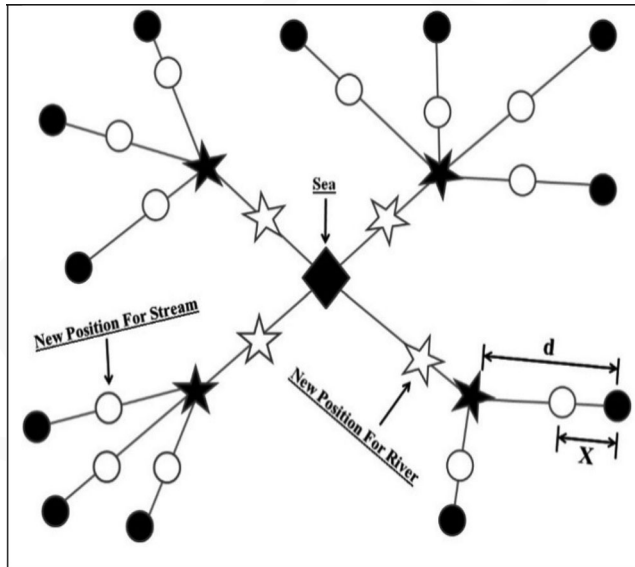


Figure 6. Schematic View of WCA.

$$NS_n = \text{round} \left\{ \left| \frac{P_n}{\sum_{i=1}^{N_{sr}} P_i} \right| \times V_{stream} \right\} \quad (8)$$

Here, NS_n presents the number of individual or streams voltage points being compared with local as well as global best points, N_{sr} and V_{stream} are

Table 1. Pseudo code of WCAfor MPPT.

```

388 1: Sense  $V_{pv}, I_{pv}$ 
389 2: Initialize  $N_{var}, N_{pop}, dist, max_{iter}, N_{sr}$ 
390 3: Randomly generate  $N_{pop}$  voltage points and calculate power  $P(V_{N_{pop}}^i)$ 
391 4: Create individual, local and global best points marked as streams, river and sea respectively
392 5: Designate streams to rivers and sea by  $NS_n = round\{\frac{P_n}{\sum_{i=1}^{N_{pop}} P_i} \times V_{stream}\}$ 
393 6: for  $i = 1 : max_{iter}$ 
394 7: %Moving streams to sea
395 8:   for  $i = NS_{sea}$ 
396 9:     generate  $V_{stream}^{j+1} = V_{stream}^j + rand \times C \times (V_{sea} - V_{stream}^j)$ 
397 10:    calculate  $P(V_{stream}^{j+1})$ 
398 11:    if  $(P(V_{stream}^{j+1}) > P(V_{sea}))$ 
399 12:       $V_{sea} = V_{stream}^{j+1}$       end end
400 13: %Moving streams to rivers
401 14:   for  $m = 1 : N_{sr} - 1$ 
402 15:     for  $k = NS_{river}^k$ 
403 16:       generate  $V_{stream}^{k+1} = V_{stream}^k + rand \times C \times (V_{river}^m - V_{stream}^k)$ 
404 17:       calculate  $P(V_{stream}^{k+1})$ 
405 18:       if  $(P(V_{stream}^{k+1}) > P(V_{river}^m))$ 
406 19:          $V_{river}^m = V_{stream}^{k+1}$       end
407 20:       if  $(P(V_{river}^m) > P(V_{sea}^i))$ 
408 21:          $V_{sea} = V_{river}^m$       end
409 22:     end end
410 23: %moving rivers to sea
411 24:   for  $j = 1 : N_{sr} - 1$ 
412 25:     generate  $V_{river}^{j+1} = V_{river}^j + rand \times C \times (V_{sea} - V_{river}^j)$ 
413 26:     calculate  $P(V_{river}^{j+1})$ 
414 27:     if  $(P(V_{river}^{j+1}) > P(V_{sea}))$ 
415 28:        $V_{sea} = V_{river}^{j+1}$       end end
416 29: %Evaporation condition and raining process
417 30:   if  $(|V_{sea} - V_{river}^j| < d_{max} \mid \text{OR} \mid V_{sea} - V_{stream}^i| < d_{max})$ 
418 31:     generate new streams using Eq. (5)      end
419 32:      $new_{sea} = V_{sea}$ 
420 33:   end
421 34: Optimum Voltage point =  $new_{sea}$ 
422 35: Calculate duty cycle

```

the total no. of local and global best points and the total number of current-voltage points.

The pseudo-code and flow chart of this technique are shown in Table 1 and Figure 7 respectively.

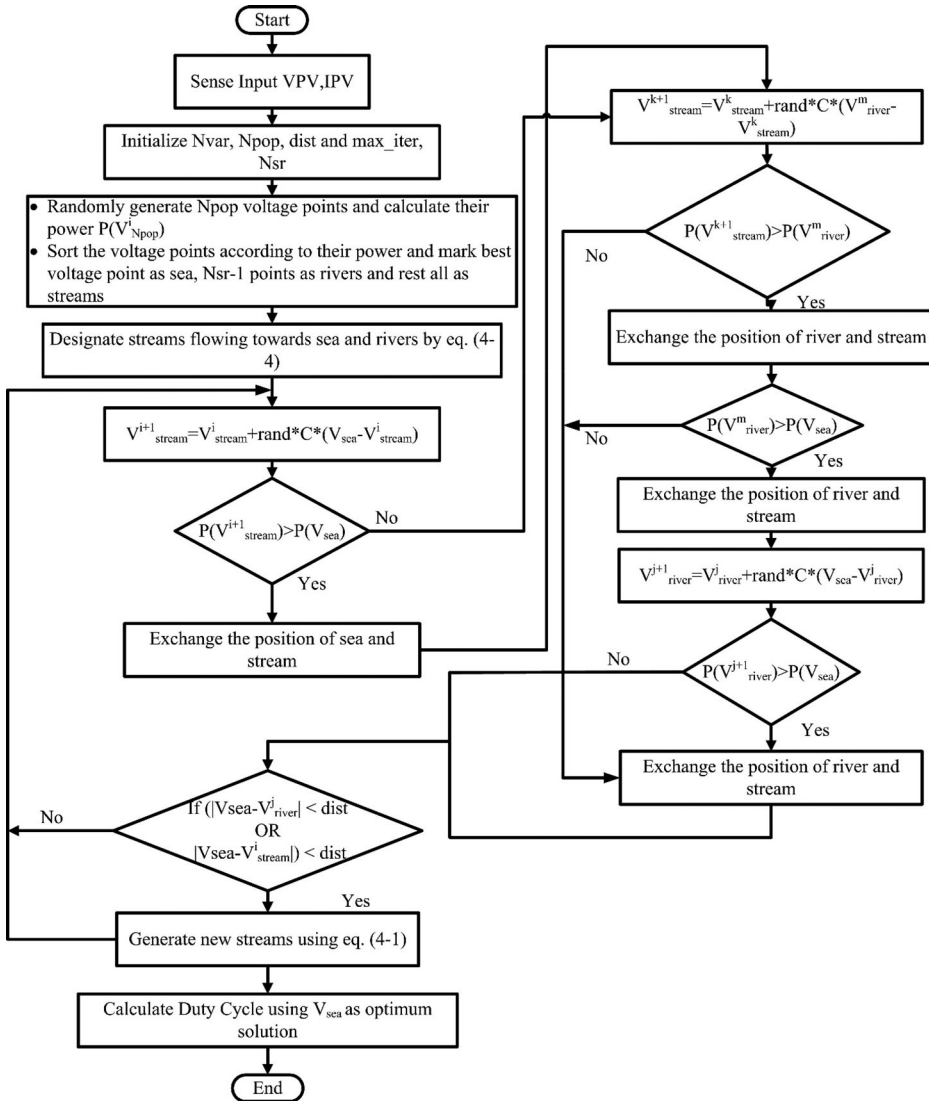
The step size of the voltage points is defined by

$$V_{stream}^{i+1} = V_{stream}^i + rand \times C \times (V_{sea}^i - V_{stream}^i) \quad C > 1 \quad (9)$$

$$V_{stream}^{i+1} = V_{stream}^i + rand \times C \times (V_{river}^i - V_{stream}^i) \quad C > 1 \quad (10)$$

$$V_{river}^{i+1} = V_{river}^i + rand \times C \times (V_{sea}^i - V_{river}^i) \quad C > 1 \quad (11)$$

V_{river} and V_{sea} are the local and global best points and V_{stream} are the current-voltage points. C is constant and if its value is more than one, then streams might flow in separate directions toward the river and the sea.



462
463
464
465
466
467
468
469
470
471
472
473

Figure 7. Flowchart of WCA based MPP Tracking.

The maximum power giving global optimum voltage point is discovered by comparing power. The position of the local best point is marked as river and the global best point is assigned as the sea in favor of a particular iteration. The individual or streams voltage points are impacted by global and local best points in subsequent iterations, and its step size is computed using Eqs. (21)–(23). The voltage at each point is located at a different location due to the step size. All the points converging into the global or sea best point with each repetition. The distance among the streams and sea comes closer to zero when the streams converge toward the MPP. To

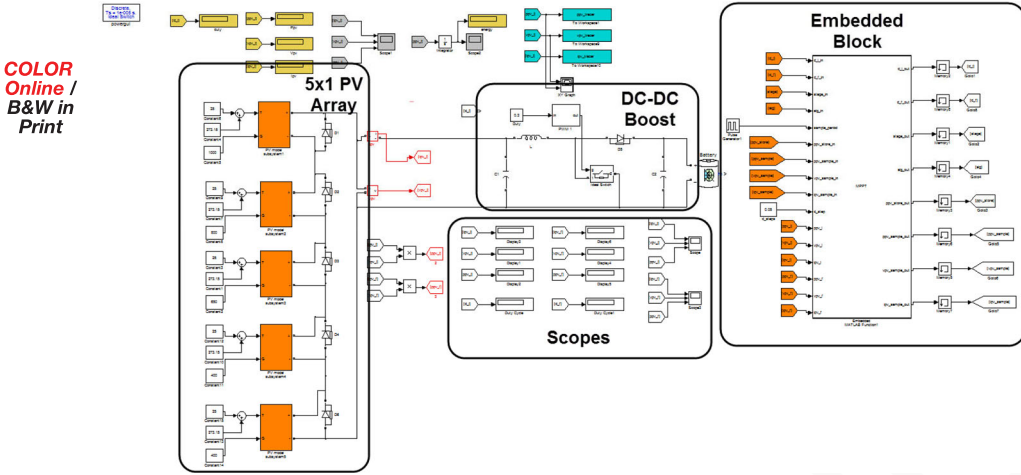


Figure 8. MATLAB/Simulink Simulation Setup.

avoid the algorithm getting stuck in the local best point a step size tolerance may be set as given below:

$$|V_{sea}^i - V_{river}^i| < dist \quad i = 1, 2, 3, \dots, N_{sr}-1 \quad (12)$$

$$|V_{sea}^i - V_{stream}^i| < dist \quad i = 1, 2, 3, \dots, NS_{sea} \quad (13)$$

Whenever the distance within the sea and a river, or sea and a stream, is below tolerance, the stream or river has entered the sea and has reached its optimal point. Then as per evaporation and precipitation phenomena, new voltage points (streams and rivers) are formed by using Eq. (19) and replaced existing streams and rivers. A larger value d_{max} decreases the search radius, whereas a small number pushes the search to be closer to the optimal point. The value for $dist$ adaptively decreases as:

$$dist^{i+1} = dist - \frac{dist^i}{\max\ iter} \quad (14)$$

$dist$ is also used as the convergence or termination criteria.

Results

Simulation Setup

MATLAB/Simulink Simulation Setup is presented in Figure 8 describes the most commonly used PV system in which the MPPT technique is implemented (Villalva et al. 2009). The setup consists of 5 series-connected solar modules and their specification is:

$P_{mpp} = 200\text{ W}$, $I_{mpp} = 7.6\text{ A}$, $V_{mpp} = 26\text{ V}$, $I_{sc} = 8.21$, $V_{oc} = 32.9\text{ V}$. The simulation setup is used to simulate and evaluate the performances of WCA, PSO, and P&O based MPP searching techniques through various PS

COLOR
Online /
B&W in
Print

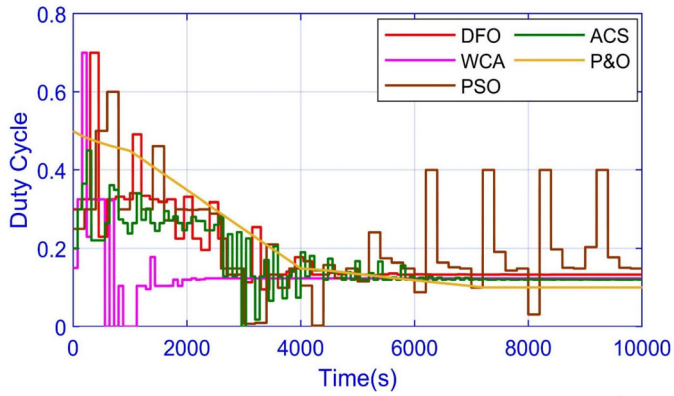


Figure 9. Case 1: Duty cycle comparability of WCA.

COLOR
Online /
B&W in
Print

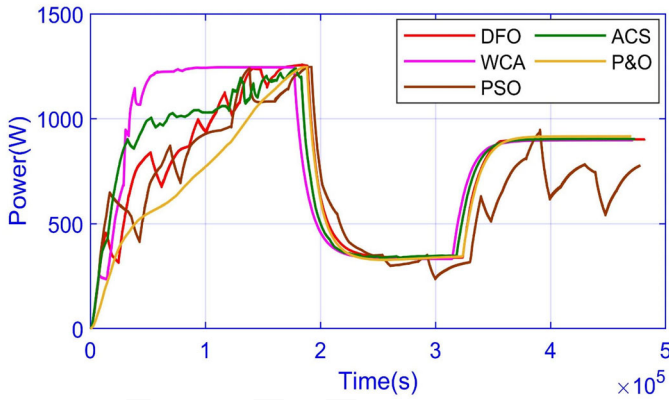


Figure 10. Case 1: Power comparability of WCA.

COLOR
Online /
B&W in
Print

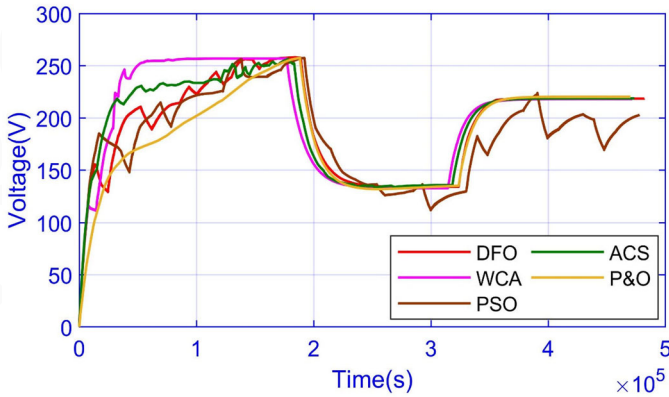
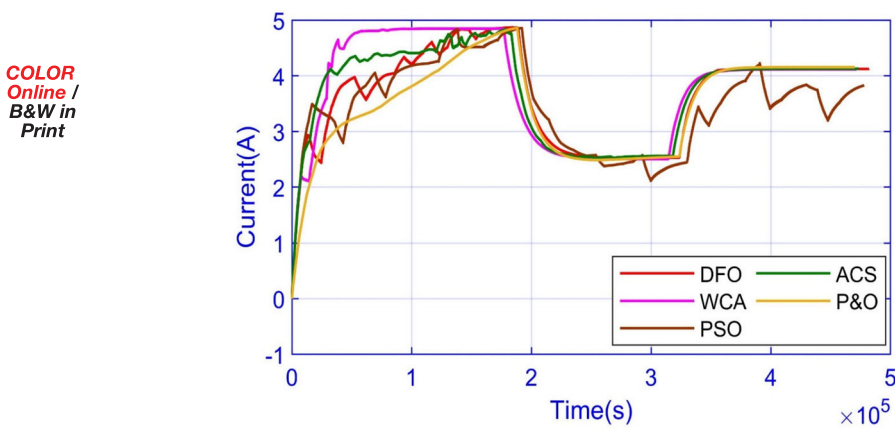
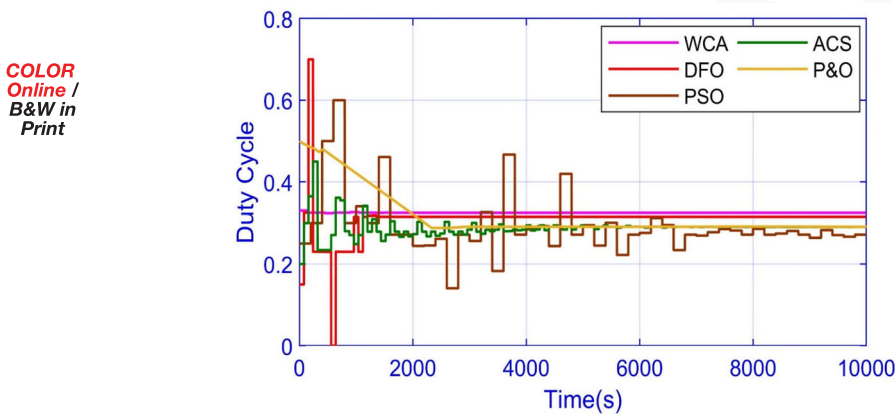


Figure 11. Case 1: Voltage comparability of WCA.

conditions. Among the battery load and PV array, the boost converter is utilized to get the required voltage as per the duty cycle. MPPT technique is implemented in the embedded block and it takes V_{pv} and I_{pv} as inputs



572 **Figure 12.** Case 1: Current comparability of WCA.



587 **Figure 13.** Case 2. Duty cycle comparability of WCA.

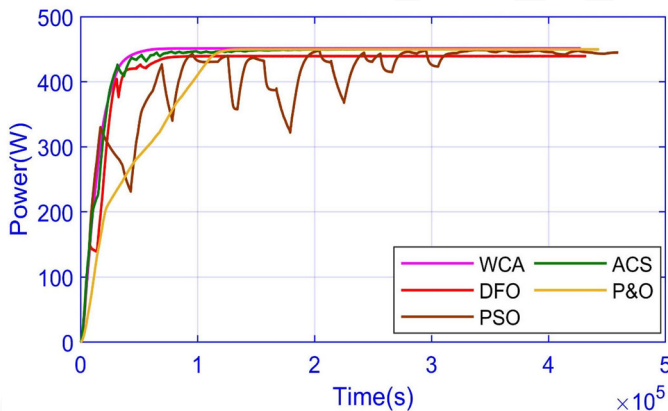
588 and D as output. Boost converter components values calculations are also
589 an important step that is worked out in (Miyatake et al. 2011). Component
590 values are as follows: $C_{in} = 10 \mu\text{F}$, $C_{out} = 47 \mu\text{F}$, $L = 200 \mu\text{H}$, $F_{sw} = 20 \text{ kHz}$.

591 The proposed technique has been tested for UI and various PS techni-
592 ques to check the accuracy and robustness. Case 1 shows the study of the
593 CVA through UI conditions in which the irradiance level is 1000 W/m^2 for
594 all 5 series-connected PV modules. Figure 13 shows the searching behavior
595 of WCA under uniform shading conditions. The proposed algorithm
596 detects the global maximum in just 28 NFEs (Number of Functions
597 evaluations = Initial population \times number of iterations) but due to the
598 raining process, it again initializes random voltage points to search for the
599 global maximum to avoid getting stuck in the local maximum until the
600 stopping criteria have been fulfilled. So the total time required to find and
601 achieve a steady state is 76 ms for WCA and 232 for PSO in case 1. For
602 uniform irradiance, searching behavior and time required to detect for all

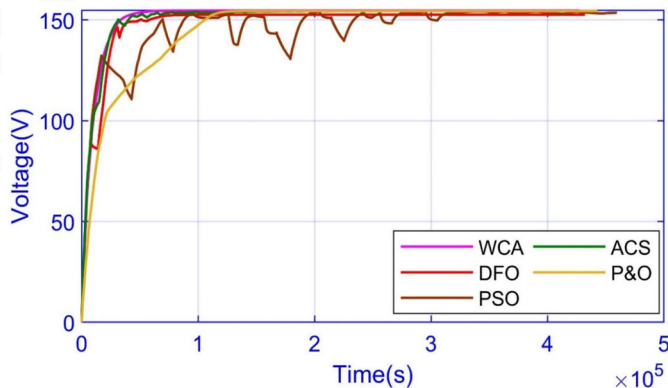
Table 2. Comparison of WCA with different partial shading algorithms.

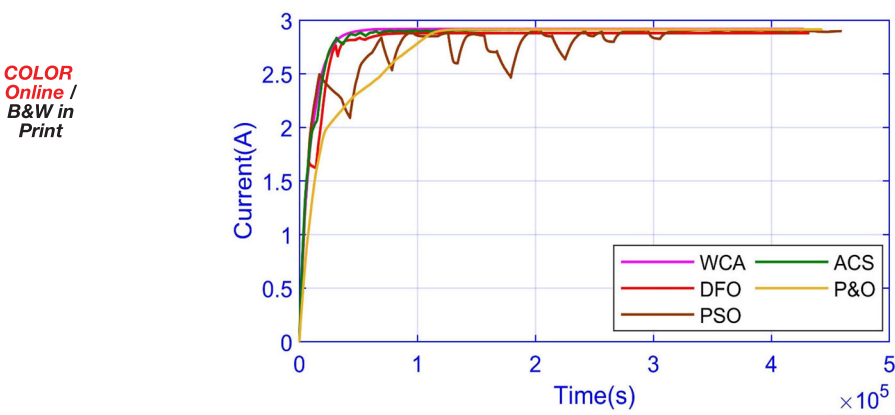
Methods	Irradiance scheme	Convergence time (s)	Settling time (s)	GM existed	GM power	Tracking power	Obtained energy	Efficiency (%)
WCA	Case1	0.17	0.20	Yes	1260	1259.3	1.66×10^3	99.8
	Case2	0.20	0.38	Yes	450	449.3	0.86×10^3	99.7
	Case3	0.20	0.25	Yes	796	794.7	1.56×10^3	99.8
	Case4	0.21	0.20	Yes	520	519.5	0.88×10^3	99.8
DFO	Case1	0.23	0.27	Yes	1260	1259.1	1.66×10^3	99.8
	Case2	0.26	0.43	Yes	450	449	0.85×10^3	99.6
	Case3	0.19	0.21	Yes	796	794.4	1.55×10^3	99.7
	Case4	0.22	0.21	Yes	520	519.2	0.87×10^3	99.7
PSO	Case1	0.47	0.70	Yes	1260	1257	1.64×10^3	94.6
	Case2	0.41	0.81	Yes	450	443	0.84×10^3	97.6
	Case3	0.68	0.71	Yes	796	791.4	1.48×10^3	99.4
	Case4	0.65	0.67	Yes	520	518.7	1.41×10^3	99.7
P&O	Case1	0.33	0.71	No	1260	1210	0.97×10^3	96.1
	Case2	0.22	0.35	Yes	450	440	1.23×10^3	97.7
	Case3	0.45	0.84	No	796	580	0.73×10^3	72.9
	Case4	0.45	0.91	Yes	520	511.3	1.39×10^3	98.2
ACS	Case1	0.47	0.64	Yes	1260	1239	1.07×10^3	98.3
	Case2	0.30	0.49	Yes	450	443	1.35×10^3	98.4
	Case3	0.39	0.81	Yes	796	790.6	1.49×10^3	99.3
	Case4	0.31	0.72	Yes	520	516.7	1.42×10^3	99.4

COLOR
Online /
B&W in
Print

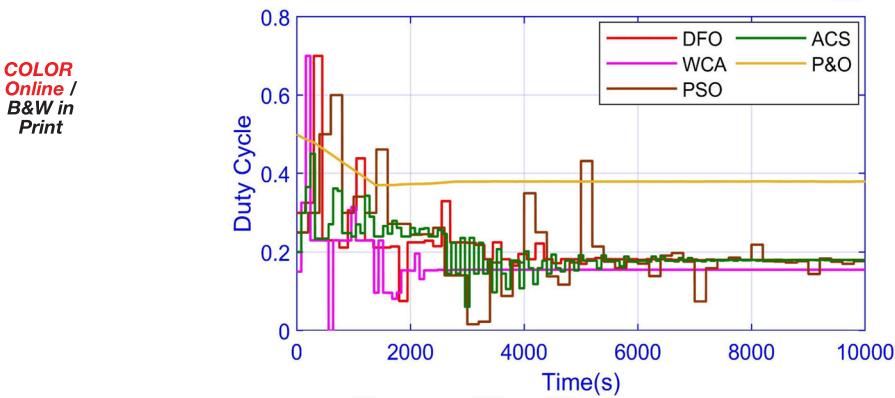
**Figure 14.** Case 2: Power comparability of WCA.

COLOR
Online /
B&W in
Print

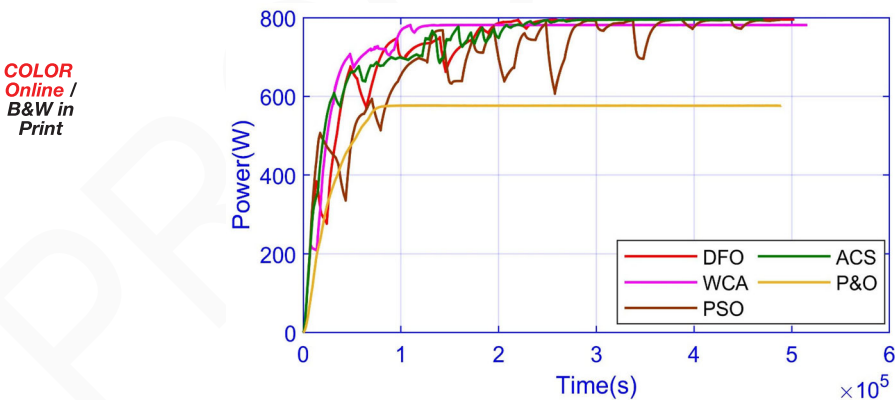
**Figure 15.** Case 2: Voltage comparability of WCA.



658 **Figure 16.** Case 2: Current comparability of WCA.



670 **Figure 17.** Case 3: Duty cycle comparability of WCA.



683 **Figure 18.** Case 3: Power comparability of WCA.

684
685
686
687
688

presented techniques are given in Figures 9 and 10. WCA is much more suitable to find global maxima than PSO because once it gets close to maxima it generates some more voltage points to ensure that the algorithm

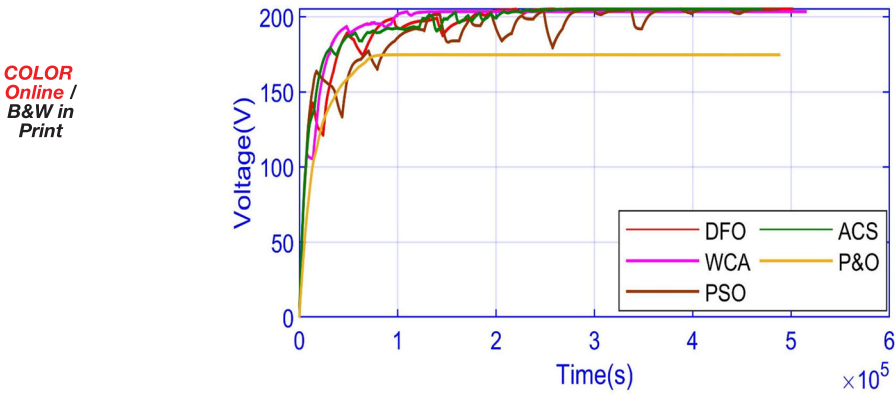
doesn't get stuck in local maxima. So the probability of WCA getting stuck in local maxima is much less than PSO which lacks exploration phenomenon and takes more time to get to global maxima. Power-time and Voltage-Time curves are shown in Figures 11 and 12 shows the searching behavior and time required to find the global maxima under partial shading techniques.

Figure 13 shows the searching behavior of WCA under shading conditions. The proposed algorithm detects the global maximum in just 28 NFEs (Number of function estimates = Initial population \times number of iterations) but due to the raining process (exploration), it again initializes random voltage points to search for the global maxima to avoid getting stuck in local maxima until stopping criteria have been fulfilled, while it takes 127 NFEs for PSO to reach MPP. So the total time required to find and achieve a steady state is 76 ms for WCA and 232 for PSO while P&O is quite fast and achieve GM in only 19 ms but it does not comes to a steady-state and keeps on oscillating which results in lower efficiency in case 1. For uniform irradiance, Power and Voltage Vs time (searching behavior) for all presented techniques are shown in Figures 9 and 10. WCA is much more suitable to find global maxima than PSO because once it gets close to maxima it generates some more random voltage points to ensure that the algorithm doesn't get stuck in local maxima. Therefore, the probability of WCA being stuck in local maxima is very less than PSO, which lack exploration phenomenon and take more time to get to global maxima. Under partially shading conditions P&O does not track GM but gets stuck in local minima. Power-time and Voltage-Time curves are shown in Figures 11 and 12, which describe the searching behavior and time, required to search the GM under PS techniques.

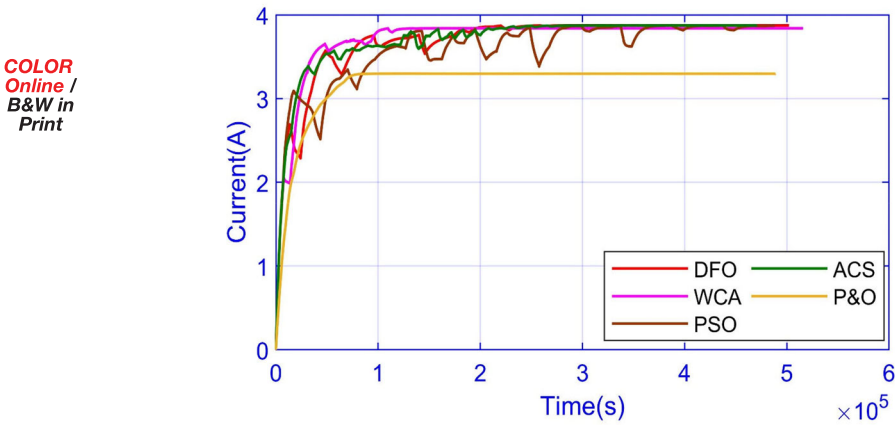
Table 2 shows the time taken to reach the global maxima and maximum power obtained by WCA, PSO, and P&O under different irradiance conditions studied in this research. The accuracy of the WCA and PSO is the same. WCA takes 76–95 ms, PSO takes 211–304 ms to reach the GM. P&O is very fast but cannot find GM. WCA presents better efficiency results as compare to PSO and P&O, WCA shows an average of 9.81% efficiency while PSO and P&O show an average of 99.67% and 62.84% efficiencies respectively. Power-Time curves of WCA under different irradiance conditions are shown in Figures 13–17. While the graphical presentation of convergence time and efficiencies of the WCA, PSO, and P&O for all uniform and partial shading cases demonstrated in Figures 18 and 19.

Case 1 (Fast Changing Irradiance)

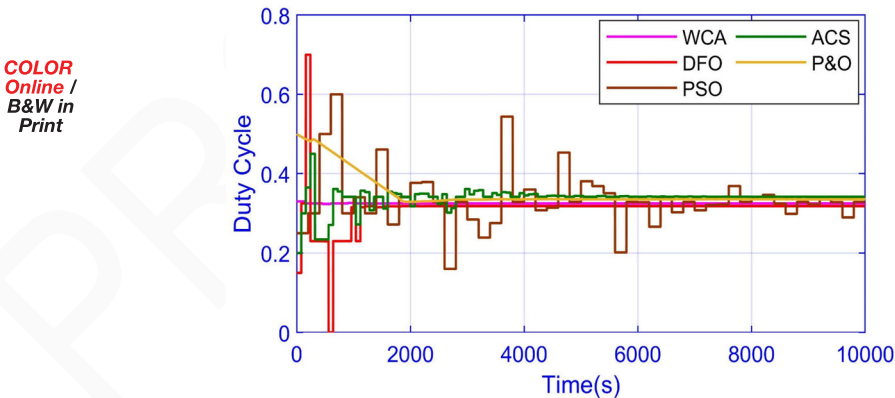
In this situation, entire PV modules have the same irradiance with rapid changing irradiance to time and their irradiance scheme is presented in Table



743 **Figure 19.** Case 3: Voltage comparability of WCA.



757 **Figure 20.** Case 3: Current comparability of WCA.

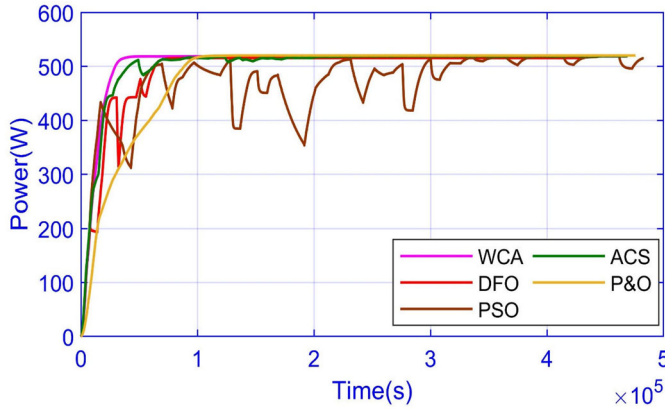


772 **Figure 21.** Case 4: Duty cycle comparability of WCA.

773
774

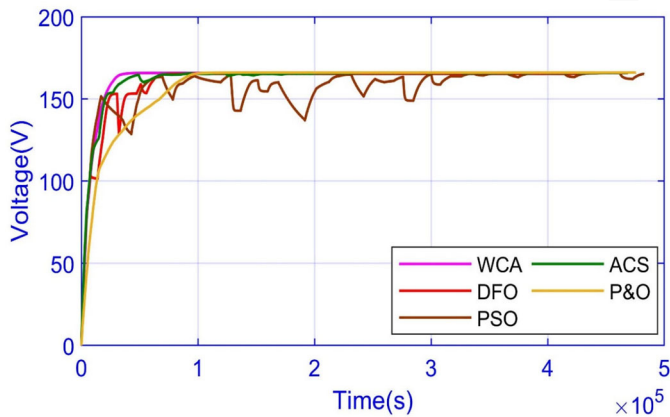
2. During the first interval, the power achieved by WCA is 1259.3 W as associated with 1259.1 W by DFO, 1257 W by PSO, 1239 W by ACS and 1210 W by P&O. WCA achieve 99.98% power-convergence efficacy in the first

775
776
777 **COLOR**
778 **Online /**
779 **B&W in**
780 **Print**



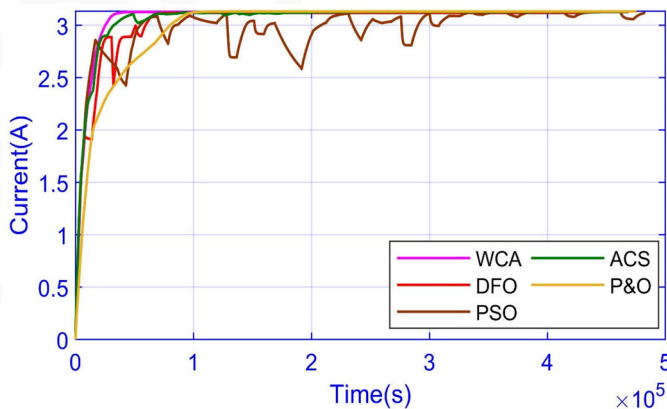
781
782
783
784
785
786
787 **Figure 22.** Case 4: Power comparability of WCA.

788
789
790 **COLOR**
791 **Online /**
792 **B&W in**
793 **Print**



794
795
796
797
798
799
800 **Figure 23.** Case 4: Voltage comparability of WCA.

801
802
803 **COLOR**
804 **Online /**
805 **B&W in**
806 **Print**



807
808
809
810
811
812
813 **Figure 24.** Case 4: Current comparability of WCA.

814 interval. Case 1 has three different regions reliant upon the irradiance magni-
815 tude. The average powers attained by WCA, DFO, PSO, ACS, and P&O are
816 830.9 W, 828.1 W, 825.1 W, 823.1 W and 819.4 W, respectively. It specifies
817

that the maximum average is attained by WCA. The average efficiency attained by the WCA, DFO, PSO, ACS, and P&O is 99.27%, 97.96%, 97.91%, 97.95%, and 98.79%. Consequently, the techniques can be hierarchical as $WCA > DFO > PSO > ACS > P\&O$. The calculated tracking time of WCA, DFO, PSO, ACS, and P&O is 0.17 s, 0.18 s, 0.46 s, 0.47 s, and 0.33 s, similarly. Settling time of WCA, DFO, PSO, ACS and P&O is 0.24 s, 0.25 s, 0.39 s, 0.64 s, 0.71 s, correspondingly. The control parameter is the duty-cycle which is present in [Figure 9](#) respectively. WCA successfully reduces the magnitude of the oscillation to is less than or equal to 1 W, achieving a 94.99% decrease in the magnitude of fluctuations. [Figure 10](#) indicates that PSO has the maximum fluctuations. ACS can harvest haphazard oscillations. The voltage and current transient are present in [Figures 11](#) and [12](#) correspondingly.

Case 2 PS (Scenario I)

In this scenario, the GMPP is at 450 W. The D, P, V, and I comparability are presented in [Figures 13–16](#) respectively. ACS and PSO show the maximum level of randomness. Settling times of ACS, PSO is large compare to WCA. Proposed technique has less oscillation in the steady-state at GMPP. The power obtained by WCA, DFO, PSO, ACS, and P&O 449.3 W, 449 W, 448 W, 443 W, and 449.5 W respectively. WCA has 99.64% efficiency as compared to DFO 99.43%, PSO 99.35%, ACS 97.93%, and P&O has 99.90%. Robustness of MPP tracking revealed by fast searching of global maxima and effective settling time at global maxima. Experimental simulations shows that it takes WCA 0.17 s, D.FO 0.19 s, P.SO 0.68 s, ACS 0.30 s and P&O 0.22 s on average and can settle after 0.55 s, 0.61 s, 0.45 s, 0.49 s and 0.35 s correspondingly. The voltage comparison result is presented in [Figure 15](#). Stable voltage and current produced by WCA is shown in [Figures 15](#) and [16](#).

Case 3 PS (Scenario II)

In this scenario the GMPP is at 796.0 W. Results for power are displayed in [Figure 18](#) and controlled delivered by the D is presented in [Figure 17](#). Voltage and current are illustrated in [Figures 19](#) and [20](#) respectively. Under PS, the MP found by WCA, DFO, PSO, ACS, and P&O are 794.7 W, 794.4 W, 785 W, 794.6 W and 580 W, respectively.

WCA achieved the highest efficiency which is 99.67%, DFO 99.54%, while the lowest efficiency achieved by P&O which is close to about 49.40% which is LM1. The tracking time of WCA is 0.175 s, dragonfly 0.180 s, PSO 0.410 s, ACS 0.390 s and P&O 0.45 s, their settling time is 0.40 s, 0.46 s, 0.56 s, 0.81 s and 0.84 s. In harvesting global maxima, WCA stands close to DFO by 12.0 ms. WCA settle at global maxima inside

455 ms achieving 19.0% faster tracking. Faster tracking improves robustness and eliminates unwanted fluctuations. WCA attains 1–4% improved efficiency of power conversion with the ripple being $<1\text{ W}$ and decreases the fluctuations to zero in the later phases of the iterative cycles. Under WCA, the output is steady, and its voltage and current have almost no fluctuations as present in Figures 19 and 20. In Figure 17, ‘D’ updating at every iteration demonstrates that WCA can sense and converge to Global Maxima in fewer iterations in appraisal to competing techniques.

Case 4 PS (Scenario III)

In this scenario, GMPP is at 520 W. The comparability is present in Figure 21 for duty-cycle. The ACS and PSO have shown extreme randomness due to random step size increments in the duty cycle. Results for power, voltage, and current are presented in Figures 22–24 respectively. Under the PS the extreme power gained by the WCA, DFO, PSO, ACS, and P&O is 519.5 W, 519.2 W, 517.6 W, 518.7 W and 519.3 W. Maximum efficiency attained by WCA is 99.80%, DFO 99.75%, PSO 97.6%, ACS 98.7% and P&O has 99.4% respectively. The tracking time to WCA, DFO, PSO, ACS, and P&O is 0.19 s, 0.25 s, 0.41 s, 0.45 s, and 0.31 s. In tracking the global maxima, WCA is closed to DFO by 10 ms. WCA settle global maxima within 453 ms attaining 18% faster tracking which enriches its robustness and also removed unwanted fluctuations. Case 4 shows the best performance among other MPPT techniques. It can perceive and converge GM in fewer iterations.

Conclusion

In this research study, a novel technique has been designed for MPPT of PV system under different irradiance conditions. Proposed MPPT technique is tested under five different irradiance conditions and under all cases, it successfully find and track the global maxima to extract maximum power from PV system. In different stages of advancement of the paper, flow charts of all presented techniques, proposed technique pseudo code and Simulink/MATLAB are also presented. Then the proposed technique is compared with other well-known and widely used conventional technique P&O and a soft computing technique PSO. After thoroughly studying the results it has been proved that proposed WCA based technique shows better results in terms of convergence speed and efficiency over P&O and PSO while accuracy is found to be same as of PSO but better than P&O. Other performance criteria like, steady state oscillations, cost and complexity is same as of PSO. WCA based technique converges in significantly less

904 time than PSO and after achieving steady state it retains zero oscillations.
905 The robustness of the WCA has been verified under uniform and various
906 partial shading conditions. WCA able to track the MPP accurately with
907 good efficiency under the partial shading conditions and shows no oscilla-
908 tion after reaching the steady state.

910 References

- 911
- 912 Aouchiche, N., M. S. Aitcheikh, M. Becherif, and M. A. Ebrahim. 2018. AI-based global
913 MPPT for partial shaded grid connected PV plant via MFO approach. *Solar Energy* 171:
914 593–603. doi:[10.1016/j.solener.2018.06.109](https://doi.org/10.1016/j.solener.2018.06.109).
- 915 Babu, T. S., N. Rajasekar, and K. Sangeetha. 2015. Modified particle swarm optimization
916 technique based maximum power point tracking for uniform and under partial shading
917 condition. *Applied Soft Computing* 34:613–24. doi:[10.1016/j.asoc.2015.05.029](https://doi.org/10.1016/j.asoc.2015.05.029).
- 918 Bouselham, L., M. Hajji, B. Hajji, and H. Bouali. 2017. A new MPPT-based ANN for
919 photovoltaic system under partial shading conditions. *Energy Procedia* 111:924–33. doi:
[10.1016/j.egypro.2017.03.255](https://doi.org/10.1016/j.egypro.2017.03.255).
- 920 Daraban, S., D. Petreus, and C. Morel. 2013. A novel global MPPT based on genetic algo-
921 rithms for photovoltaic systems under the influence of partial shading. IECON
922 **Q2** Proceedings (Industrial Electronics Conference), 1490–1495.
- 923 Daraban, S., D. Petreus, and C. Morel. 2014. A novel MPPT (maximum power point track-
924 ing) algorithm based on a modified genetic algorithm specialized on tracking the global
925 maximum power point in photovoltaic systems affected by partial shading. *Energy* 74
(C):374–88. doi:[10.1016/j.energy.2014.07.001](https://doi.org/10.1016/j.energy.2014.07.001).
- 926 Eskandar, H., A. Sadollah, A. Bahreininejad, and M. Hamdi. 2012. Water cycle algorithm -
927 A novel metaheuristic optimization method for solving constrained engineering opti-
928 mization problems. *Computers and Structures* 110–111:151–66. doi:[10.1016/j.compstruc.](https://doi.org/10.1016/j.compstruc.2012.07.010)
929 [2012.07.010](https://doi.org/10.1016/j.compstruc.2012.07.010).
- 930 Ghaffarzadeh, N. 2015. Water Cycle Algorithm based power system stabilizer robust design
931 for power systems. *Journal of Electrical Engineering* 66 (2):91–6. doi:[10.1515/jee-2015-](https://doi.org/10.1515/jee-2015-0014)
932 [0014](https://doi.org/10.1515/jee-2015-0014).
- 933 Ghasemi, M. A., H. M. Foroushani, and M. Parniani. 2016. Partial shading detection and
934 smooth maximum power point tracking of PV arrays under PSC. *IEEE Transactions on*
Power Electronics 31 (9):6281–92. doi:[10.1109/TPEL.2015.2504515](https://doi.org/10.1109/TPEL.2015.2504515).
- 935 Haroon, S. S., and T. N. Malik. 2017. Short-term hydrothermal coordination using water
936 cycle algorithm with evaporation rate. *International Transactions on Electrical Energy*
937 *Systems* 27 (8):1–18.
- 938 Harrag, A., and S. Messalti. 2015. Variable step size modified P&O MPPT algorithm using
939 GA-based hybrid offline/online PID controller. *Renewable and Sustainable Energy*
940 *Reviews* 49:1247–60. doi:[10.1016/j.rser.2015.05.003](https://doi.org/10.1016/j.rser.2015.05.003).
- 941 Ishaque, K., Z. Salam, A. Shamsudin, and M. Amjad. 2012. A direct control based max-
942 imum power point tracking method for photovoltaic system under partial shading condi-
943 tions using particle swarm optimization algorithm. *Applied Energy* 99:414–22. doi:[10.](https://doi.org/10.1016/j.apenergy.2012.05.026)
944 [1016/j.apenergy.2012.05.026](https://doi.org/10.1016/j.apenergy.2012.05.026).
- 945 Karami, N., N. Moubayed, and R. Outbib. 2017. General review and classification of differ-
946 ent MPPT Techniques. *Renewable and Sustainable Energy Reviews* 68:1–18. doi:[10.1016/j.](https://doi.org/10.1016/j.rser.2016.09.132)
[rser.2016.09.132](https://doi.org/10.1016/j.rser.2016.09.132).

- 947 Miyatake, M., M. Veerachary, F. Toriumi, N. Fujii, and H. Ko. 2011. Maximum power
948 point tracking of multiple photovoltaic arrays: A PSO approach. *IEEE Transactions on*
949 *Aerospace and Electronic Systems* 47 (1):367–80. doi:10.1109/TAES.2011.5705681.
- 950 Mohapatra, A., B. Nayak, P. Das, and K. B. Mohanty. 2017. A review on MPPT techniques
951 of PV system under partial shading condition. *Renewable and Sustainable Energy*
952 *Reviews* 80:854–67. doi:10.1016/j.rser.2017.05.083.
- 953 Punitha, K., D. Devaraj, and S. Sakthivel. 2013. Artificial neural network based modified incre-
954 mental conductance algorithm for maximum power point tracking in photovoltaic system
955 under partial shading conditions. *Energy* 62:330–40. doi:10.1016/j.energy.2013.08.022.
- 956 Ram, J. P., T. S. Babu, and N. Rajasekar. 2017. A comprehensive review on solar PV max-
957 imum power point tracking techniques. *Renewable and Sustainable Energy Reviews* 67:
958 826–47. doi:10.1016/j.rser.2016.09.076.
- 959 REN21. 2018. Renewables 2018 Global Status Report [Online]. [http://www.ren21.net/wp-](http://www.ren21.net/wp-content/uploads/2018/06/17-8652_GSR2018_FullReport_web_final_.pdf)
960 [content/uploads/2018/06/17-8652_GSR2018_FullReport_web_final_.pdf](http://www.ren21.net/wp-content/uploads/2018/06/17-8652_GSR2018_FullReport_web_final_.pdf) (accessed
961 December 26, 2018).
- 962 Sadollah, A., H. Eskandar, A. Bahreininejad, and J. H. Kim. 2015. Water cycle algorithm
963 for solving multi-objective optimization problems. *Soft Computing* 19 (9):2587–603. doi:
964 10.1007/s00500-014-1424-4.
- 965 Q3 Villalva, M. G., J. R. Gazoli, and E. R. Filho. 2009. Modeling and circuit-based simulation
966 of photovoltaic arrays. 1244–54.
- 967 Villalva, M. G., J. R. Gazoli, and E. R. Filho. 2009. Comprehensive approach to modeling
968 and simulation of photovoltaic arrays. *IEEE Transactions on Power Electronics* 24 (5):
969 1198–208. doi:10.1109/TPEL.2009.2013862.
- 970 Yilmaz, U., A. Kircay, and S. Borekci. 2018. PV system fuzzy logic MPPT method and PI
971 control as a charge controller. *Renewable and Sustainable Energy Reviews* 81:994–1001.
972 doi:10.1016/j.rser.2017.08.048.
- 973 Zhang, J., K. Ding, R. Mei, and Y. Cai. 2018. Global maximum power point tracking
974 method based on sorting particle swarm optimizer. *International Journal of Green Energy*
975 15 (13):821–36. doi:10.1080/15435075.2018.1529579.
- 976
977
978
979
980
981
982
983
984
985
986
987
988
989